IASJ المجلات الاكاديمية العراقية

Tikrit Journal of Pure Science

ISSN: 1813 – 1662 (Print) --- E-ISSN: 2415 – 1726 (Online)

Journal Homepage: http://tjps.tu.edu.iq/index.php/j

The effect of band offsets of absorption layer on CNTS / ZnS / ZnO solar cell by SCAPS-1D

Hardan T. Ganem , Ayed N. Saleh

Department of physics, Collage of Education for pure science, Tikrit University, Tikrit, Iraq

https://doi.org/10.25130/tjps.v25i6.316

ARTICLE INFO.

Article history:

-Received: 26 / 7 / 2020

-Accepted: 15 / 9 / 2020

-Available online: / / 2020

Keywords: SCAPS-1D, Simulation solar cells CNTS, band offsets of absorption.

Corresponding Author:

Name: Hardan T. Ganem

E-mail:

hardanganem@gmail.com

ayed.ns@tu.edu.iq

Tel:

ABSTRACT

The ZnO/ZnS/ CNTS solar cell was studied using SCAPS-1D simulation. The cell efficiency was 9.38% and to improve the cell a back reflection layer (BSL) was added, so the conversion efficiency increased to 10.65% and we entered buffer layers, thus the cell structure became ZnO / Buffer / CNTS the conversion efficiency increased to 10.78%. It turns out that the effect of the buffer layer is greater than the reflection layer. The best cell was ZnO/CdS/CNTS/Cu_2O and the conversion efficiency was 12.09%, fill factor 62.98%, short circuit current 20.01 mA/cm^2 finally open circuit voltage 0.95V.

Introduction

Semiconductors absorb photons that have more energy than the forbidden energy gap and lose excess energy by thermal, radioactive, or non-radioactive processes, there are efforts to increase their efficiency by achieving the manufacture of various solar cells [1]. The interest of researchers for several decades brought the use of compounds (CIGS), (CdTe) in the manufacture of thin films of solar cells because these materials are characterized by high efficiency and in return. Their cost is high and occupies a wide area, some are rare and others are toxic, so researchers sought to replace them with other materials, and they found alternative materials such as (CZTS) compound and they are non-toxic and available and possess good electrical and optical properties and can study new compounds and that by replacing (Zn) with elements (Ni, Fe, Cd, Be, Mg, Mn) and other elements called Chalcogenide quaternary they available in the Earth's crust low cost when produced are non-toxic and have energy gaps close to the ideal value and have a high absorption coefficient [2 , 3]. Therefore, increased interest in these materials and their excellent optical and electrical properties for making thin films.

The compound Cu_2NiSnS_4 (CNTS) is one of the important compounds because of its distinctive characteristics, as it possesses a direct energy gap (1.45-1.74eV). It is close to the ideal gap and is available in the earth's crust, non-toxic, p-type, has a high absorption coefficient and has the ability to absorb the spectrum Solar and the compound can be prepared using a spin coating or dipping coating and other methods, so it is one of the candidate compounds for the manufacture of solar cells [4,5]. We will in this research study (CNTS) Copper, nickel, tin and sulfur as a absorption layer and compare the experimental results with the simulation results and the possibility of improving the characteristics of the cell through add a back reflection layer and buffer layer to get a highly efficient cell.

Modeling

Numerical simulation SCAPS

Modeling can be done using the SCAPS program, a one-dimensional solar cell simulation program designed at the University of Gent in Belgium to simulate traditional crystalline materials for semiconductor CIGS and CdTe. The user can describe a cell with a maximum of seven layers for different properties such as optical absorption, thickness, doping concentrate, energy gap and other. The spectral responses are determined and can be

calculated in the dark and in the light. This program has been developed and applied to all solar cells. It is a freely available program. The program depends on solving Poisson equation [6].

$$\nabla(E) = \frac{q}{\varepsilon}(p - n + N_D^+ - N_A^-) \ldots.1$$

Where q is elementary charge, E is the electrical field, n is density of electrons, p is density of holes, ε is the permittivity of the absorber, N_D is donor concentration and N_A acceptor concentration.

Then the continuity equation that is given by equation [7].

$$\frac{dn}{dt} = \frac{1}{q}(\nabla(J_n) + G_n - R_n \ldots.2$$

$$\frac{dp}{dt} = -\frac{1}{q}(\nabla(J_p) + G_p - R_p \ldots..3$$

Where G_n is electron generation rate ,G_p is hole generation rate, J_n is electron current density , J_p hole current density , R_n is electron recombination rate and R_p hole recombination rate.

The charge carrier equations for diffusion and drift current can be obtained from the following equations [8].

$$J_n = q(\mu_n nE + D_n \nabla n) \ldots..4$$

$$J_p = q(\mu_p PE + D_p \nabla p) \ldots..5$$

Where D is the diffusion constant, μ_n (μ_p) is Electron (hole) mobility.

To measure the quality of the photovoltaic cells the fill factor FF, short circuit current J_{sc}, voltage circuit open V_{oc} and conversion efficiency η as these variables are related to each other with the following equations [8].

$$FF = \frac{P_{max}}{P_t} = \frac{V_{\max} . I_{max}}{Voc . J_{sc}} \quad \ldots..6$$

$$\eta = \frac{P_m}{P_{in}} = \frac{Voc.Jsc . FF}{P_{in}} \quad \ldots\ldots7$$

It can be determined the age of minority carriers which is the average time needed to recombine minority carriers and is associated with the traps and recombine with the following relationship [9].

$$\tau = \frac{1}{\sigma V_{th} N_t} \ldots\ldots8$$

$$\tau = \frac{\Delta n}{R} \ldots\ldots.9$$

Where N_t is defects concentration, τ is minority carrier life time, V_{th} is Thermal speed, R is recombination rate, Δn is excess minority carrier concentration and σ is conductivity.

Solar cell structure

The CNTS / ZnS / ZnO solar cell is composed of the ZnO window layer of transparent metal oxides having a relatively large energy gap, then followed by the ZnS buffer layer and has a suitable energy gap for the absorption layer gradation with penetration, and then the CNTS absorption layer that has a relatively small energy gap. The front and back contact is Ohmic so that we get the lowest energy loss [10]. The cell shall be on the ground of the glass. Table (1) the defect values to be entered in the absorption layer of the SCAPS program to study the cell performance and table (2) gives the values of the program parameters and We took the series resistance (4.76 Ωcm^2) and the shut resistance (980 Ωcm^2) and the temperature (300 k). Figure (1) shows the structure of the solar cell**.**

flat bands (front)
ZnO Windows Layer
buffer Layer ZnS
absorption Layer CNTS
(back) flat bands
glass

Fig. 1: The installation of solar cells.

To enhance the efficiency of solar cells the following facts must be addressed:

- Adding different layers of back reflection to increase cell efficiency.
- Adding various buffer layers to improve cell performance.

Combine the best reflection layers with the best buffer layers to get the best cell.

Table 1: defects value in the cell.

Defect properties	Interface defect p-CNTS/n-ZnS
Energy level with respect to reference (eV)	0.6
Total density Nt (cm^{-2})	1.0× 10 ^{12}
Capture cross section area of electrons (cm^2)δ_e	1.0× 10 $^{-15}$
Capture cross section area of holes (cm^2)δ_h	1.0× 10 $^{-15}$

Table 2: Physical parameters for the basis cell layers.

Parameters	symbol (unit)	CNTS [11]	ZnS [12]	ZnO [7]
Thickness	W(μm)	4	0.1	0.1
Bandgap	Eg (ev)	1.74	3.3	3.3
Electron affinity	χ (ev)	3.87	4.4	4.5
Dielectric permittivity	ε_r	9	10	9
CB effective density of states	$N_C(cm^{-3})$	2.2× 10^{18}	1.8× 10^{18}	2.2× 10^{18}
VB effective density of states	$N_V(cm^{-3})$	1.8× 10^{19}	1.8× 10^{19}	1.8× 10^{19}
Electron thermal velocity	V_n(cm/s)	1.0× 10^7	1.0× 10^7	1.0× 10^7
Hole thermal velocity	V_P(cm/s)	1.0× 10^7	1.0× 10^7	1.0× 10^7
Electron mobility	$\mu_n (cm^2/v.s)$	11	100	100
Hole mobility	$\mu_p (cm^2/v.s)$	11	25	25
Shallow uniform donor density	N_D (1/cm^3)	0	1.0× 10^{15}	1.0× 10^{15}
Shallow uniform acceptor density	N_A (1/cm^3)	1.0× 10^{17}	0	0

Result and discussion

Device optimization

The solar cell was simulated to achieve the optimum performance of CNTS solar cells by analyzing the energy diagram and adding a number of layers of back reflection and buffer layers with changing the doping rates of the layers added to achieve the best performance.

Energy band diagram

The CNTS / ZnS / ZnO solar cell energy diagram is given in figure (2) in the presence of light and it has been obtained through the SCAPS program. Through the diagram, it is possible to see the gap separation from the CNTS absorption layer due to the valance band offsets (VBO) between CNTS/ZnS while the movement of electrons at the back contact is stopped by the effect of the conduction band offsets (CBO) at the absorption layer. The energy gap of the absorption layer is within the visible spectrum, which increases the amount of energy-absorbed photons.

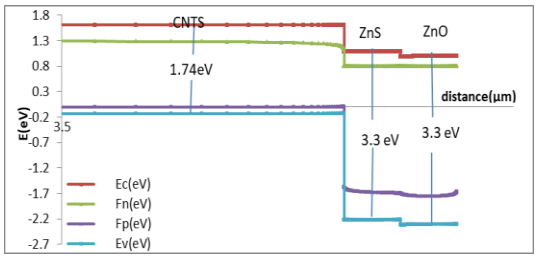

Fig. 2: Energy band diagram.

J-V dark and light characteristics of solar cell

The program was run in the dark and light, to know the characteristic of the diode and figure (3) shows the properties of the curve (I-V) because the dark current is very small and is a result of the thermal activation energy of the minority carriers. When lighting the solar cell creates an electron-hole pair from incident photons that have energy of equal to the energy gap of the solar cell.

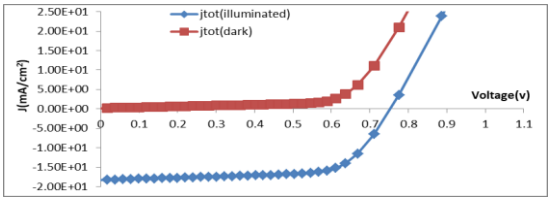

Fig. 3: Dark and illuminated (J-V) of photovoltaic cell.

3-2- The effect of the back reflection layer

In order to further improve the studied cell ZnO / ZnS / CNTS we study the effect of adding different layers of reflection back (BSL) and consist of the following compounds ($MoSe_2$, SnS, CdTe, Si, ZnTe, Cu_2O, CuO, $CuSbS_2$, MoS_2, CISe, CIGS , CZTS, CZTSe, CFTS, CBTS , CZTSSe, and Cu_2Te) we stabilize cell parameters and then add the back reflection layers with the doping concentrate changed only and figure (4,a) shows the conversion efficiency of cell different reflection layers that the best back reflection layers are (Cu_2O, CBTS , ZnTe) the reason for the emergence of a positive conduction band offsets between the reflection and absorption layer In the form of spike that prevents recombination and increases cell efficiency [9]. Then the efficiency begins with a gradual descending. Electron affinity and the energy gap are important parameters that determine the conduction band offsets if there is a cliff between the absorption reflections layer the cell performance decreases. The conduction band offsets can be found by the following equation.

$$CBO = \Delta E_c = \chi_{Absorbers} - \chi_{\text{Reflection}} \quad \ldots.10$$

Where $\chi_{Absorbers}$ and $\chi_{\text{Reflection}}$ is electron affinity absorbers and reflection and CBO (ΔE_c) is conduction band offsets.

There is a second equation to find the valance band offsets

$$VBO = \Delta E_v = \left[\chi_{Absorber} + E_{g(Absorber)}\right] - \left[\chi_{\text{Reflection}} + E_{g(Reflection)}\right] \ldots.11$$

The figure (4,a) represents the values of the energy gap and the electron affinity, so we note that the reflection layers that have more energy gap than the energy gap of the absorption layer (conduction band), they have higher efficiency. CFTS generates a small value Spike compared to Cliff, so its efficiency will decrease, and as we have shown previously Cliff reduces cell performance. Other layers have Cliff and cell efficiencies decrease as Cliff increases. Figure (4,b) which shows the of the electron affinity and the energy gap for all materials. Figure (4,c) shows the conduction band offsets and valance band offsets. Table (3) shows the physical parameters of the different layers of the back reflection.

Table 3: The physical parameters of the different layers of the back reflection

Parameters	symbol (unit)	$MoSe_2$ [13]	SnS [14]	CdTe [15]	Si [16]	ZnTe [17]	Cu_2O[18]	CuO [18	CuSbS2 [19]	MoS2 [20]	CISe [21]	CIGS [22]
Band gap	Eg (ev)	1.060	1.1	1.45	1.12	2.19	2.17	1.51	1.5	1.7	1	1.05
Electron affinity	χ (ev)	4.372	4.2	4.28	4.05	3.73	3.2	4.07	4.5	4.2	4.5	4.14
Dielectric permittivity	ε_r	13.6	12.5	9.4	11.9	10.3	7.11	18.1	10	13.6	13.6	10
CB effective density of states	$N_C(cm^{-3})$	2.2×10^{18}	1.0×10^{19}	7.5×10^{17}	2.58×10^{19}	1.17×10^{18}	2.0×10^{17}	2.2×10^{19}	2.2×10^{18}	2.2×10^{18}	2.2×10^{18}	1.0×10^{18}
VB effective density of states	$N_V(cm^{-3})$	1.8×10^{19}	4.13×10^{19}	$1.8\times 10_{19}$	2.65×10^{19}	1.16×10^{19}	1.1×10^{19}	5.5×10^{20}	1.8×10^{19}	1.8×10^{19}	1.8×10^{18}	1.0×10^{18}
Electron thermal velocity	V_n(cm/s)	1.0×10^7	1.0×10^7	1.0×10^7	1.0×10^7	3.2×10^7	1.0× 107	1.0×10^7	1.0×10^7	1.0× 107	1.0×10^7	1.0×10^7
Hole thermal velocity	V_P(cm/s)	1.0×10^7	1.0×10^7	1.0×10^7	1.0×10^7	1.5×10^7	1.0×10^7	1.0×10^7	1.0×10^7	1.0×10^7	1.0×10^7	1.0×10^7
Electron mobility	$\mu_n (cm^2/v.s)$	100	25	500	1350	330	200	100	100	100	40	30
Hole mobility	$\mu_p (cm^2/v.s)$	25	100	60	450	80	80	0.1	25	25	10	15
Shallow uniform donor density	N_D (1/cm^3)	0	0	0	0	0	0	0	0	0	0	0
Shallow uniform acceptor density	N_A (1/cm^3)	1.0×10^{15}	1.0×10^{22}	1.0×10^{21}	1.0×10^{22}	1.0×10^{20}	1.0×10^{19}	1.0×10^{22}	1.0×10^{20}	1.0×10^{20}	1.0×10^{20}	1.0×10^{22}

Table Supplement (3)

Parameters	symbol (unit)	CZTS [23]	CZTSe [23]	CFTS [24]	CBTS [7]	CZTSSe [12]	Cu_2Te [25]
Bandgap	Eg (ev)	1.5	0.95	1.3	1.9	1.3	1.18
Electron affinity	χ (ev)	4.5	4.35	3.3	3.6	4.1	4.2
Dielectric permittivity	ε_r	10	13.6	9	5.4	13.6	10
CB effective density of states	$N_C(cm^{-3})$	2.2×10^{18}	2.2×10^{18}	2.2×10^{18}	2.2×10^{18}	2.2×10^{18}	7.8×10^{17}
VB effective density of states	$N_V(cm^{-3})$	1.8×10^{19}	1.8×10^{18}	1.8×10^{19}	1.8×10^{19}	1.8×10^{19}	1.6×10^{19}
Electron thermal velocity	V_n(cm/s)	1.0×10^7	1.0×10^7	1.0×10^7	1.0×10^7	1.0×10^7	1.0×10^7
Hole thermal velocity	V_P(cm/s)	1.0×10^7	1.0×10^7	1.0×10^7	1.0×10^7	1.0×10^7	1.0×10^7
Electron mobility	$\mu_n (cm^2/v.s)$	100	100	21.98	30	100	500
Hole mobility	$\mu_p (cm^2/v.s)$	25	25	21.98	10	25	100
Shallow uniform donor density	N_D (1/cm^3)	0	0	0	0	0	0
Shallow uniform acceptor density	N_A (1/cm^3)	1.0×10^{20}	1.0×10^{22}	1.0×10^{22}	1.0×10^{20}	1.0×10^{22}	1.0×10^{22}

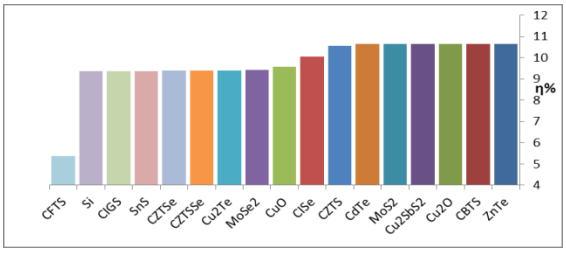

Fig. 4, a: Shows the conversion efficiency of cell different reflection materials.

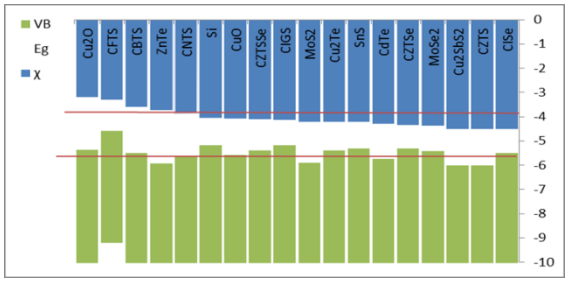

Fig. 4, b: Shows the sum of the electronic affinity and the energy gap for all materials.

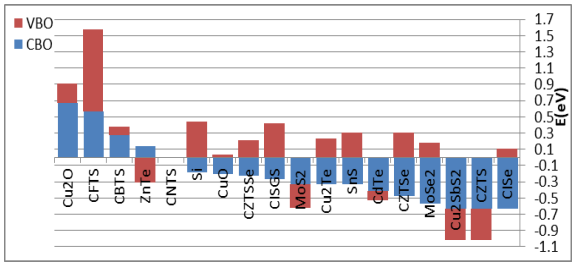

Fig. 4, c: Offsets of conduction and valance band values after adding the back reflection layer

The effect of the buffer layer

Various buffer layers were added to the improved cell after ZnO / ZnS / CNTS as the cell parameters stabilized, so the change will only be in the buffer layer in layer type and impurity concentration. It turned out that the buffer layer had a significant effect on the properties of the cell due to the large difference in the energy gap between the absorption and window layers [26]. And compounds that were added as an buffer layer (SiC, V_2O_5, TiO_2, ZnSe, CdS, In_2S_3) were the best buffer layers (TiO_2, V_2O_5, CdS) the reason for the high efficiency of CdS, V_2O_5 and TiO_2 to be the negative conduction band offsets which helps to return electrons and increase efficiency [27]. Table (4) shows the basic parameters of the buffer layer and figure (5,a) show offsets conduction and valance band values after adding the buffer layer and figure (5,b) the values of the electronic affinity and the energy gap for the various buffer material. It appears that the buffer layers constitute with the absorption layer a cliff in the conduction band offsets that possesses a large conversion efficiency, especially if the conduction band offsets of the medium-value as in CdS. But that the conduction band offsets is less than the window layer is Its efficiency is very low as shown in figure (5,c) for SiC energy band diagram and the figure (5,d) shows conversion efficiency after adding the buffer layers and the cell structure as follows ZnO / ZnS / Buffer / CNTS.

Table 4: The physical parameters of the different layers of the buffer.

Parameters	symbol (unit)	TiO_2 [24]	CdS [28]	In_2S_3 [20]	ZnSe [29]	V_2O_5 [25]	SiC [30]
Band gap	Eg (ev)	3.2	2.4	2.8	2. 9	2.3	2.3
Electron affinity	χ (ev)	3.86	4.5	4.7	4.09	3.99	3.8
Dielectric permittivity	ε_r	9	9	13.5	10	4.28	9.72
CB effective density of states	$N_C(cm^{-3})$	1.8×10^{19}	1.8×10^{19}	2.2×10^{17}	1.5×10^{18}	2.2×10^{18}	4.8×10^{15}
VB effective density of states	$N_V(cm^{-3})$	2.4×10^{18}	2.4×10^{18}	1.8×10^{19}	1.8×10^{19}	1.8×10^{19}	3.2×10^{15}
Electron thermal velocity	V_n(cm/s)	1.0×10^{7}	1.0×10^{7}	1.0×10^{7}	1.0×10^{7}	1.0×10^{7}	1.0×10^{7}
Hole thermal velocity	V_P(cm/s)	1.0×10^{7}	1.0×10^{7}	1.0×10^{7}	1.0×10^{7}	1.0×10^{7}	1.0×10^{7}
Electron mobility	$\mu_n (cm^2/v.s)$	100	100	100	50	1.26	900
Hole mobility	$\mu_p (cm^2/v.s)$	25	25	25	20	34.5	40
Shallow uniform donor density	N_D ($1/cm^3$)	1.0×10^{17}	1.0×10^{21}	1.0×10^{22}	1.0×10^{17}	1.0×10^{17}	1.0×10^{21}
Shallow uniform acceptor density	N_A ($1/cm^3$)	0	0	0	0	0	0

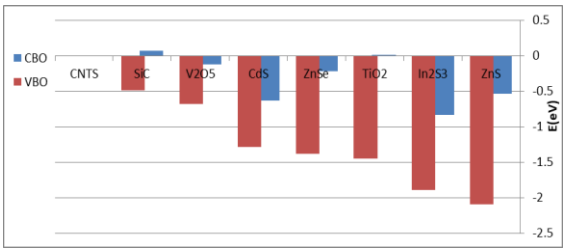

Fig. 5,a: Offsets conduction and valance band values after adding the buffer layer.

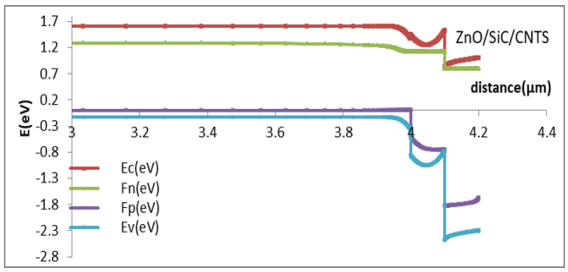

Fig. 5, c: Energy band diagram of SiC layer.

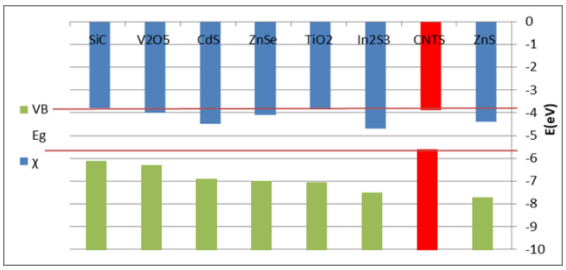

Fig. 5, b: Shows the sum of the electronic affinity and the energy gap for all materials.

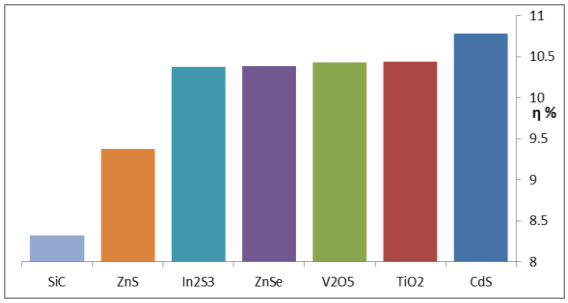

Fig. 5, d: The conversion efficiency of all cells after the addition of the buffer layer.

The results of the buffer and reflection layers

To obtain the best cells we simulate the buffer layers (V_2O_5, CdS, In_2S_3, ZnSe, ZnTe, and $TiO_{2)}$ with the all back reflection layers. Figure (6) results obtained from simulation and it is shown that cells containing CdS buffer layer have high conversion efficiency and the worst efficiency that have SiC buffer layer.

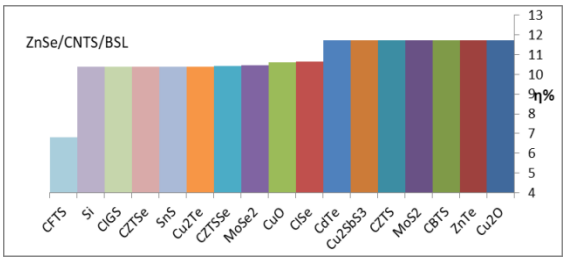

Fig.6, a: Results of solar cells after adding all the BSL with ZnSe layer.

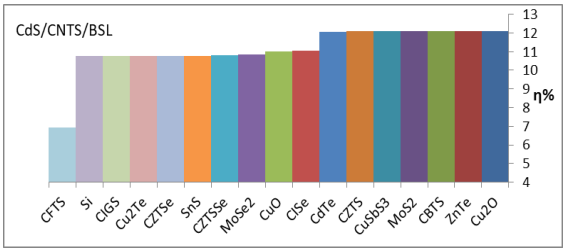

Fig. 6, b: Results of solar cells after adding all the BSL with CdS layer.

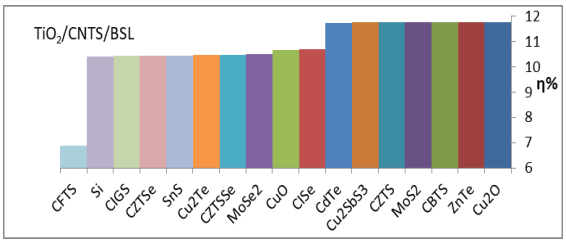

Fig. 6, c: Results of solar cells after adding all the BSL with TiO_2 layer.

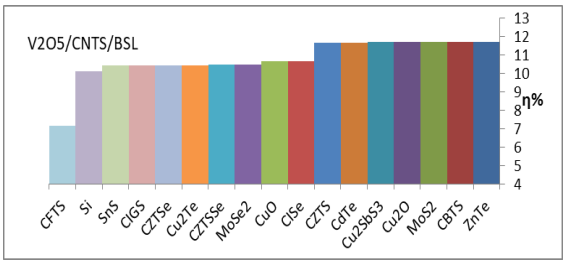

Fig. 6, d: Results of solar cells after adding all the BSL with V_2O_5 layer.

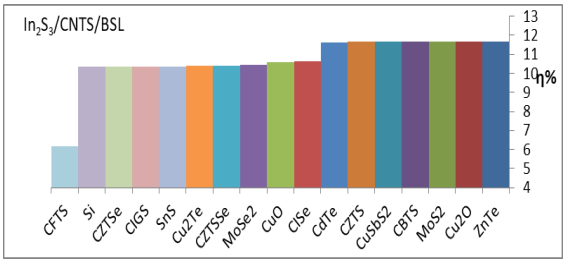

Fig. 6, e: Results of solar cells after adding all the BSL with In_2S_3 layer.

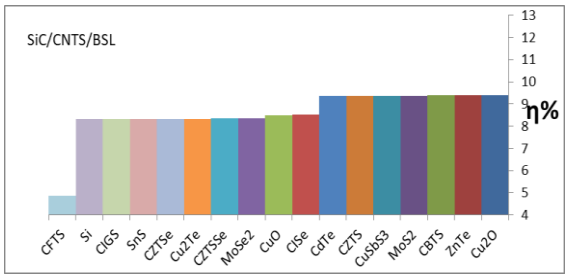

Fig. 6, F: Results of solar cells after adding all the BSL with SiC layer.

Study the properties of the best resulting cells: Comparison of the properties of Curve (J-V)

To study the properties of a current voltage curve we enter the parameters of each cell on the SCAPS program. The comparison of cells in table (7) that show how to improve the efficiency of the solar cell it shows a comparison between Cell before optimization and the cell parameters by adding the best back reflection layer Cu_2O and then the best cell by adding a buffer layer CdS and finally represents the best cell after adding the Cu_2O back reflection layer and CdS buffer layer and figure (7) shows the relationship of voltages with current for all cells in table (5) those values.

Table 5: Theoretical cells and the best results obtained from the study.

S	Cell	V(v)	J(ma/cm^2)	FF %	η %
1.	ZnO/ZnS/CNTS	0.75	18.28	67.92	9.38
2.	ZnO/ZnS/CNTS/Cu_2O (BSL)	0.75	20.66	67.92	10.65
3.	ZnO/ZnS/CdS/CNTS (Buffer)	0.93	18.01	63.93	10.78
4.	ZnO/ZnS/CdS/CNTS/Cu_2O	0.95	20.01	62.98	12.09

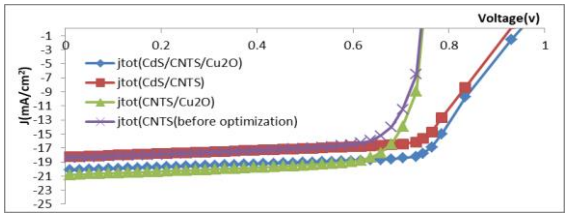

Fig. 7: The reaction of current with voltage for several cells.

Energy diagram

We notice from figure (8) the four states of the energy level shows the states of the conduction band and the valence band with a Fermi level of electrons and holes and we note the gradient of the window and buffer layer because the electron affinity and the energy gap for both layers are converging and we notice. The first case as in figure (8,a) Cliff between the absorption and buffer layer conduction band due to the difference of the electron affinity and the energy gap between them and as shown in table (1). The second case as shown in figure (8, b) higher potential barrier will be generated between the two contacting layers and varies according to the type of the two layers and the parameters of the layers, so the positive conduction band offsets (+ CBO) it occurs in which the back reflection is Spike than the absorption layer and this leads to an decrease in recombination. This leads to the return of electrons reduces

recombination and increases the efficiency of the solar cell. The three case as shown in figure (8, c) when adding a layer of buffer that creates Cliff in the energy diagram leads to an increase in the number of holes because it reflects the holes and returns them to the absorption layer so that it increases the conversion efficiency [4]. The last case as in figure (8, d) showing energy levels. When the cell is add reflection and buffer layers ZnO / CdS / CNST / Cu_2O will appear Cliff between CNTS/CdS and spike between Cu_2O/CNTS due to the affinity and energy gap.

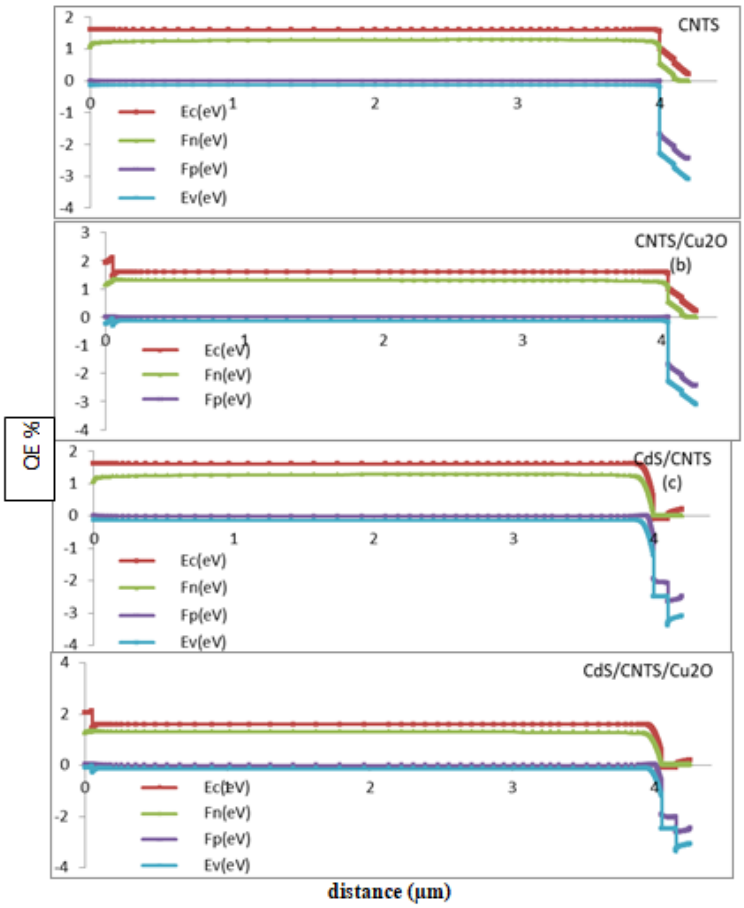

Fig. 8: Energy diagram (a) Cell before optimization (b) The cell after adding the reflection layer (c) The cell after adding an buffer layer (d) The cell after adding the reflection and buffer layer.

Quantum Efficiency

The number of pairs of electron- hole caused by the light falling on the cell. Figure (9) shows the quantum efficiency and its relationship to the wavelength of the best cells obtained. We find that the absorption is small at wavelengths less than 380 nm for cells that have the CdS buffer layer and the reason for this is to recombination the front surface which reduces the absorption of light and absorption in the CdS layer due to its small energy gap compared to the other layers but the quantum efficiency becomes 90% at the wavelength of 385 nm and then begins the gradual descending. As for the back reflection cell and the cell before addition, the quantum efficiency is 90% until reaches 380 nm and then increases to become 100% due to the gradual increase in the spectral response, because the spectral response increases as the wavelength increases, according to the following relationship. [31]

$$R_\lambda = \frac{QE\,.\lambda}{1.24} \quad -----12$$

Where R_λ is spectral response, and QE is Quantum efficiency.

The quantum efficiency is zero at long wavelengths. so no light below the energy gap can be absorbed.

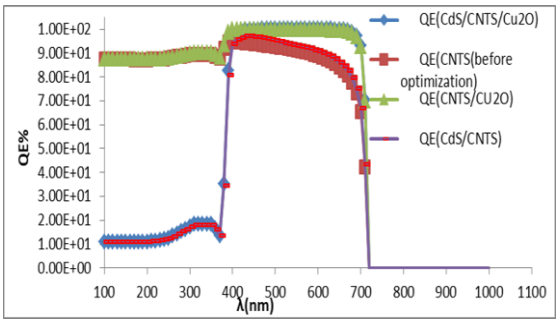

Fig. 9: Quantum efficiency as a function of the wavelength of the best studied cells.

Conclusions

The ZnO / ZnS / CNTS cell was simulated by SCAPS. then we entered different layers of reflection on the cell ZnO / ZnS / CNTS / BSL showing an

increase in the conversion efficiency from 9.38% to 10.65% then add different buffer layers between the absorption and window layers ZnO / buffer / CNTS the conversion efficiency has increased 10.78% then we introduced the layers BSL with the buffer layers shows the best of these cells ZnO / CdS / CNTS / Cu_2O and conversion efficiency 12.09%.

Acknowledgement

The research was supported reviewed and reviewed by the Scientific Committee of the Department of Physics, College of Education for Pure Sciences, Tikrit University.

References

[1] Skhouni, O.et al. (2017). Boosting the Performance of Solar Cells with Intermediate Band Absorbers the Case of ZnTe: O. *Journal of Energy and Power Engineering*, 11:417-426.

[2] Simya, O.K.et al. (2014). Dye-sensitized solar cells based on visible-light-active TiO_2 heterojunction nanoparticles. *Synthetic metals*, 188:124-129.

[3] Sarkar, S.et al. (2018). Flower-like Cu_2NiSnS_4 microspheres for application as electrodes of asymmetric supercapacitors endowed with high energy density. *CrystEngComm*, 20(10):1443-1454.

[4] Khattak, Y.H.et al. (2018). Effect of Cu_2O hole transport layer and improved minority carrier life time on the efficiency enhancement of Cu_2NiSnS_4 based experimental solar cell. *Journal of Renewable and Sustainable Energy*, 10(4):043502.

[5] Wang, T.X. et al. (2014). Flower-like Cu_2NiSnS_4 nanoparticles synthesized by a facile solvothermal method. *Materials Letters*, 124: 148-150.

[6] Skhouni, O. et al. (2016). Numerical study of the influence of ZnTe thickness on CdS/ZnTe solar cell performance. *The European Physical Journal Applied Physics*, 74(2):24602.

[7] Hameed, K.Y. et al. (2019). Modelling of novel-structured copper barium tin sulphide thin film solar cells. *Bulletin of Materials Science*, 42(5):.231.

[8] Ganvir, R. (2016). Modelling of the nanowire CdS-CdTe device design for enhanced quantum efficiency in Window-absorber type solar cells. .University of Kentucky.

[9] Baig, F. (2019). Numerical analysis for efficiency enhancement of thin film solar cells. Ph.D. thesis, Instituto de Diseño para la Fabricación, Universitat Politècnica de València, Spain: 164pp

[10] Like .S. M. (1990) .The localization of both .Ghaleb, F. and Ahmed, H. A. Physics and Technology of Semiconductor Devices, *Al-Hikma House for Printing and Publishing*, Mosul. (In Arabic).

[11] Khattak, Y.H. (2019). CZTSe Kesterite as an Alternative Hole Transport Layer for $MASnI_3$ Perovskite Solar Cells. *Journal of Electronic Materials*, 48(9):.5723-5733.

[12] Cherouana, A. and Labbani, R. (2017). Study of CZTS and CZTSSe solar cells for buffer layers selection. *Applied Surface Science*, 424:.251-255.

[13] Minbashi, M.et al.(2017). Comparison of theoretical and experimental results for band-gap-graded CZTSSe solar cell. *Current Applied Physics*, 17(10): 1238-1243.

[14] Omrani, M. K.et al. (2018). Improve the performance of CZTSSe solar cells by applying a SnS BSF layer. *Solid-State Electronics*, 141: 50-57.

[15] Anuforonini, G. and Duduyemi, O. (2016). Simulation of the performance of CdTe/CdS/ZnO multi-junction thin film solar cell. *Simulation*, 3(1):1-10.

[16] Boumaour, M. et al. (2019). High efficiency silicon solar cells with back ZnTe layer hosting IPV effect: a numerical case study. *Journal of Taibah University for Science*, 13(1):696-703.

[17] Bayad, H.et al. (2018). Influence of P+-ZnTe back surface contact on photovoltaic performance of ZnTe based solar cells. *Optical and Quantum Electronics*, 50(6):259.

[18] Sawicka-Chudy, P., Sibiński, M., Wisz, G., Rybak-Wilusz, E. and Cholewa, M., (2018),. Numerical analysis and optimization of Cu_2O/TiO_2, CuO/TiO_2, heterojunction solar cells using SCAPS. In *Journal of Physics: Conference Series* ,1033(1): 012002.

[19] Olopade, M.et al. (2017). The Study of Some Materials as Buffer Layer in Copper Antimony Sulphide ($CUSbS_2$) Solar Cell Using SCAPS 1-D. In *2017 IEEE 44th Photovoltaic Specialist Conference (PVSC)*: 2381-2384

[20] Rafee Mahbub, M.et al. (2016). Simulation of CZTS thin film solar cell for different buffer layers for high efficiency performance .*ENGINEERING AND TECHNOLOGY*, 2(52): 1-10.

[21] Nichterwitz, M.et al. (2013). Generation-dependent charge carrier transport in Cu (In, Ga) Se2/CdS/ZnO thin-film solar cells. *Journal of Applied Physics*, 113(4):044515.

[22] Löckinger, J.et al. (2018). TiO_2 as intermediate buffer layer in Cu (In, Ga) Se_2 solar cells. *Solar Energy Materials and Solar Cells*, 174:397-404.

[23] Simya, O. K. Mahaboobbatcha, A. and Balachander, K. (2015). A comparative study on the performance of Kesterite based thin film solar cells using SCAPS simulation program. *Superlattices and Microstructures*, 82: 248-261.

[24] Khattak, Y.H.et al. (2018). Numerical modeling baseline for high efficiency (Cu_2FeSnS_4) CFTS based thin film kesterite solar cell. 164: 547-555.

[25] Najim, A. H. & Saleh, A. N. (2019). Study effect of window and BSF layers on the properties of the CZTS/CZTSe solar cell by SCAPS–1D. *Tikrit Journal of Pure Science*, 24(3): 77-83.

[26] Eisele, W.et al. (2003). XPS, TEM and NRA investigations of Zn (Se, OH)/Zn (OH) 2 films on Cu

(In, Ga)(S, Se) $_2$ substrates for highly efficient solar cells. *Solar energy materials and solar cells*, 75(1-2): 17-26.
[27]Martin, A. Crane translation by Hassan, Y. M. (1989). Solar Cells Principles of Work, Technology and System Applications. *Baghdad National Library*. (In Arabic)
[28] Khattak, Y.H.et al. (2018). Effect of CZTSe BSF and minority carrier life time on the efficiency enhancement of CZTS kesterite solar cell. *Current Applied Physics*, 18(6): 633-641.
[29] Olopade, M. A.et al. (2012). Investigation of some materials as buffer layer in copper zinc tin sulphide (Cu_2ZnSnS_4) solar cells by SCAPS-1D. *Advances in Applied Science Research*, 3(6): 3396-3400.
[30] Zerfaoui, H.et al. (2019). The simulated effects of different light intensities on the SiC-based solar cells. *Silicon*, 11(4):1917-1923.
[31] Ghania, A. (2012). THEME STUDY OF SILICON SOLAR CELLS PERFORMANCES USING THE IMPURITY PHOTOVOLTAIC EFFECT. M. Sc. THESE .Université Ferhat Abbas–Setif la Faculté des Sciences Département de Physique.Algérienne.

تأثير ازاحة حزمة طبقة الامتصاص على الخلية الشمسية CNTS / ZnS / ZnO باستخدامSCAPS-1D

حردان ذياب غانم , عايد نجم صالح

قسم الفيزياء , كلية التربية للعلوم الصرفة , جامعة تكريت , تكريت , العراق

الملخص

تمت دراسة الخلية الشمسية ZnO / ZnS / CNTS باستخدام محاكاة SCAPS-1D. وكانت كفاءة الخلية 9.38٪ ، ولتحسين الخلية تم إضافة طبقة انعكاس خلفي (BSL) ، لذلك زادت كفاءة التحويل إلى 10.65٪ ، ودخلنا طبقات موائمة فأصبحت تركيب الخلية ZnO / Buffer / CNTS زادت كفاءة التحويل إلى 10.78٪ . اتضح أن تأثير الطبقة العازلة أكبر من طبقة الانعكاس. وان أفضل خلية تم الحصول عليها ZnO / CdS / CNTS / Cu_2O وكانت كفاءة التحويل 12.09% ، عامل التعبئة 62.98% ، تيار الدائرة القصيرة 20.01 mA/cm^2 واخيراً فولتية الدائرة المفتوحة0.95 V.